JAST (Journal of Animal Science and Technology) TITLE PAGE

Upload this completed form to website with submission

ARTICLE INFORMATION	Fill in information in each box below
Article Type	Research article
Article Title (within 20 words without abbreviations)	Functional characteristics of a pig 2D intestinal organoid model as an in vitro platform for nutritional studies
Running Title (within 10 words)	Characteristics of pig organoid models for nutritional research
Author	Sang Seok Joo1, Bon-Hee Gu2, Eunbyeol Lee1, Eunseon Oh3, Minji Kim4, Hyunjung Jung4, Myunghoo Kim1,5,*
Affiliation	1 Department of Animal Science, College of Natural Resources & Life Science, Pusan National University, Miryang 50463, Korea 2 Life and Industry Convergence Research Institute, Pusan National University, Miryang 50463, Korea 3 Application Center, CJ Blossom Park, Suwon 16495, Korea 4 Animal Nutrition and Physiology Division, National Institute of Animal Science, Rural Development Administration, Wanju 55365, Korea 5 Institute for Future Earth, Pusan National University, Busan 46241, Korea
ORCID (for more information, please visit https://orcid.org)	Sang Seok Joo (https://orcid.org/0000-0001-8909-1102) Bon-Hee Gu (https://orcid.org/0000-0001-7368-3074) Eunbyeol Lee (https://orcid.org/0009-0009-6615-8840) Eunseon Oh (https://orcid.org/0009-0007-3766-1805) Minji Kim (https://orcid.org/0000-0003-2106-1921) Hyunjung Jung (https://orcid.org/0000-0002-7004-2017) Myunghoo Kim (https://orcid.org/0000-0002-8444-6952)
Competing interests	No potential conflict of interest relevant to this article was reported.
Funding sources State funding sources (grants, funding sources, equipment, and supplies). Include name and number of grant if available.	This research was funded by a 2-Year Research Grant of Pusan National University.
Acknowledgements	Not applicable.
Availability of data and material	Upon reasonable request, the datasets of this study can be available from the corresponding author.
Authors' contributions Please specify the authors' role using this form.	Conceptualization: Joo SS, Kim M (Myunghoo Kim). Data curation: Joo SS, Gu BH. Formal analysis: Joo SS, Gu BH, Lee E. Methodology: Joo SS, Gu BH, Kim M (Minji Kim). Software: Oh E, Kim M (Minji Kim). Validation: Jung HJ, Kim M (Myunghoo Kim) Investigation: Joo SS, Lee E, Oh E. Writing - original draft: Joo SS, Lee E, Kim M (Myunghoo Kim). Writing - review & editing: Joo SS, Gu BH, Lee E, Oh E, Kim M (Minji Kim), Jung HJ, Kim M (Myunghoo Kim).
Ethics approval and consent to participate	The experimental protocols describing the management and care of animals were reviewed and approved by the Animal Care and Use Committee of Chungbuk National University, Cheongju, Korea (approval#CBNUA-1421-20-02).

CORRESPONDING AUTHOR CONTACT INFORMATION

For the corresponding author (responsible for correspondence, proofreading, and reprints)	Fill in information in each box below
First name, middle initial, last name	Myunghoo Kim
Email address – this is where your proofs will be sent	mhkim18@pusan.ac.kr
Secondary Email address	
Address	Department of Animal Science, College of Natural Resources & Life Science, Pusan National University, Miryang 50463, Korea
Cell phone number	+82-10-3082-3598
Office phone number	+82-55-350-5803
Fax number	+82-55-350-5519

Abstract

Intestinal epithelial cell lines have been widely used in the field of biomedical and livestock research, and recently, the use of organoid systems has been attempted. However, they have several limitations as an in vitro platform in particularly in nutrition-related studies. Thus, this study aimed to compare the existing in vitro platform (IPEC-J2 cell line) with a three-dimension (3D) organoid model, and to understand the nutritional phenomena occurring in the intestinal lumen through the establishment and characterization of a two-dimension (2D) organoid model. By comparing the IPEC-J2 cell line and 3D intestinal organoids, we found differences in intestinal epithelial cell types, including nutrient-related enteroendocrine cells and enterocytes. 3D organoids have most of gut epithelial cell types, but IPEC-J2 did not. We further established a 2D organoid model with an exposed apical membrane and compared it with a 3D organoid model. The established 2D organoids had higher expression of enteroendocrine cells and enterocyte marker genes, and most genes were related to nutritional properties (nutrient transporters, hormones, and digestive enzymes). Fatty acids, one of the nutrients, were added to the two organoid models for comparison. Fluorescence image analysis confirmed that more fatty acids were absorbed by 2D organoids. Treatment with a long-chain fatty acid mixture increased the expression of fatty acid receptor (*FFAR1* and *FFAR4*) and hormone (*GCG*, *CCK*, and *PYY*) genes in 2D organoids but not in 3D organoids, leading to the activation of metabolic responses. The more facilitated metabolic process was observed in 2D organoids by increased mitochondria activity and ATP production. Our findings emphasize that pig intestinal organoid systems, particularly 2D organoid model, is better in vitro platform, particularly in nutrition-related studies. Compared with other in vitro platforms, 2D organoids can be used for studying intestinal epithelial cell-nutrient interactions structurally and characteristically. Our study provides a basis for utilizing a pig 2D intestinal organoid model as a potentially advanced in vitro system for intestinal epithelial cell-based nutritional research in domestic animals.

Keywords: Pig organoids, 2D organoid model, Nutrition, Enteroendocrine cells, Enterocytes

Introduction

Pigs are one of the major livestock, with pork accounting for more than a quarter of the total protein consumed worldwide and approximately 35% of the total meat production [1]. Pigs are recognized as important livestock, and various studies are being conducted to increase their productivity. The health status of pigs is influenced by a combination of multiple factors, including genetics, environmental stress, pathogen infection, and nutrition [2-4]. Among these factors, nutrition is particularly related to gut health, and numerous studies have focused on enhancing

gut health in pigs. For example, positive indicators related to gut health, such as reduced diarrhea incidence, increased tight junction protein gene expression, and improved intestinal morphology, were identified when plant-derived oils rich in n-3 polyunsaturated fatty acids were fed to weaned piglets as feed additive [5]. In contrast, an in vitro study using the pig intestinal epithelial cell line, IPEC-J2, examined the effects of functional nutrients on gut health. For example, acetate and propionate enhance cell viability and gut barrier integrity [6].

Recently, because of animal welfare issues, methods that can replace animal experiments have attracted considerable attention. However, in vitro studies in domestic animals are limited. Organoid culture systems can mimic and reproduce tissue functions and properties. For example, organoid systems are highly similar to living organisms and can be applied in genetic engineering, making them economically and efficiently suitable for high-throughput screening [7]. In addition, organoids have the characteristics of cell populations related to organs, which enables the study of interactions with factors related to these organs. A representative example is the intestinal organoid-based co-culture system used in mechanistic studies [8]. In a study by Hou et al., an organoid-based co-culture model with lamina propria immune cells isolated from the intestine was developed, and the immune cell-epithelium regulatory mechanism of *Lactobacillus reuteri*, a well-known probiotic, was investigated. Thus, organoid-based co-culture models are recognized as advanced tools with the potential for in vitro research on biological processes [9, 10]. Intestinal organoids can be generated using embryonic, pluripotent, and adult stem cells [11]. These stem cells can be cultured under appropriate culture medium conditions without a specific feeder cell [12]. For example, isolated crypts, which contain adult stem cells, undergo self-renewal, organization, morphogenesis, and differentiation within the crypt-villus structure [13]. Crypt-derived intestinal organoids exhibit structural and functional similarities to the gut.

Recently, various intestinal organoids have been developed for livestock, including cattle, sheep, chicken, and pigs [14-17]. Many studies have investigated intestinal diseases induced by pathogenic microbes and viruses in pig gut organoids. Disease-inducing microbes such as *Salmonella typhimurium* and *Toxoplasma gondii* can directly infect pig organoids [18]. In a study by Li et al., a transmissible gastroenteritis virus, a pig enteric coronavirus, was found to infect pig jejunal organoids. In a previous study, apical-out and two-dimension (2D) culture methods were used due to structural limitations in three-dimension (3D) culture, which is the basic organoid culture method [19]. Pathogens mainly infect the intestinal lumen, and most nutrient uptake and sensing occurs in the intestinal lumen, resulting in metabolic processes. Thus, the 2D organoid model has several advantages as an in vitro research platform because it can simulate phenomena occurring in the intestinal lumen.

Although studies on pig intestinal organoids have been actively conducted, the characteristics of these platforms remain unclear. Therefore, this study aimed to compare the characteristics of the existing pig intestine in vitro platform with pig organoids, and to establish a 2D organoid model for better intestinal epithelial cell research. A 2D organoid model was developed to simulate external exposure of the lumen using pig 3D organoids, and the physiological and nutritional characteristics were compared. Our results suggest the possibility of using the 2D pig organoid model in nutritional research.

Materials and Methods

Cell culture

IPEC-J2, a pig intestinal cell line, was kindly provided by Prof. Yun of Seoul National University. IPEC-J2 cells were cultured in a 90 mm cell culture dish (SPL Life Sciences, Pocheon, Korea) using DMEM/F12 medium (Thermo Fisher Scientific, Waltham, MA, USA), supplemented with 10% fetal bovine serum, 100 U/mL penicillin, and 100 μg/mL streptomycin (Thermo Fisher Scientific) at 37 °C in a humidified 5% CO_2 atmosphere. For RNA extraction and immunofluorescence staining, 5×10^5 cells were seeded to 6-well plates (SPL Life Sciences) and 35 mm confocal dishes (SPL Life Sciences) for 2 days.

R-spondin 1 and Wnt-3a are critical factors in pig intestinal organoids. To procure them, two cell lines expressing the target proteins were used in cell culture-conditioned media. Conditioned media were prepared as described previously [20]. Briefly, R-spondin 1-expressing HEK293T cells and L Wnt-3A cells (CRL-2647™, ATCC, Manassas, VA, USA) were cultured in a 90 mm cell culture dish using DMEM medium (Thermo Fisher Scientific), supplemented with 10% fetal bovine serum, 100 U/mL penicillin, and 100 μg/mL streptomycin, with selective antibiotics for 2-3 passages. The selective antibiotics used were: 0.2 mg/mL Hygromycin B (Thermo Fisher Scientific) for HEK 293T cells and 0.4 mg/mL G-418 (Thermo Fisher Scientific) for L Wnt-3A cells. To obtain a high concentration of conditioned media, the cells were initially cultured (5×10^5 cells in a 90 mm cell culture dish) for 7 days using advanced DMEM/F12 medium (Thermo Fisher Scientific) with 10% fetal bovine serum, 100 U/mL penicillin, and 100 μg/mL streptomycin. Briefly, cells were grown for 4 days (approximately 8-90% confluence at this point) in harvest media (first batch). The medium was replaced with fresh culture medium, and the cells were cultured for another 3 days in the harvest media (second batch). Finally, the first and second batches were mixed and filtered in a 1:1 ratio and stored at -20 °C until further use.

Isolation of pig small intestinal crypts for organoid culture

In this study, three jejunal fragments were harvested from 3-week-old weaned piglets, all of which were healthy and asymptomatic. For crypt isolation, 3-4 cm of the gut tissue was harvested and opened longitudinally. To remove luminal contents and mucus, they were gently scraped using slide glass and vigorously washed with phosphate-buffered saline (PBS, Thermo Fisher Scientific). The gut tissues were then cut to 0.5 × 0.5 cm^2 pieces and transferred to a crypt isolation solution containing 30 mM ethylene-diamine-tetra acetic acid (EDTA, Thermo Fisher Scientific) and 1 mM DL-dithiothretiol (DTT, Sigma-Aldrich, St. Louis, MO, USA). The tissue fragments were incubated for 30 min on ice in a horizontal shaking incubator at 100 rpm. After incubation, the tissue fragments were transferred to a cold crypt washing buffer containing 54.9 mM D-sorbitol (Sigma-Aldrich) and 43.4 mM sucrose (Sigma-Aldrich) in PBS, and gently shaken for 2 min to release the crypts. To obtain pure crypts, the supernatant was transferred to a new tube using 100 μm cell strainer (SPL Life Sciences) and centrifuged at 200 × *g* for 5 min. The crypt pellet was resuspended in advanced DMEM/F12 medium and counted for pig intestinal organoid culture.

Culture and maintenance of pig intestinal organoids

The counted pig jejunal crypts were mixed with advanced DMEM/F12 and Matrigel (Corning Inc., Corning, NY, USA) in a 1:1 ratio. The mixture was seeded into a 96-well cell culture plate (SPL Life Sciences) at a concentration of 5 crypts/μL (total volume: 4 μL). The plate was then incubated for 30 min in a cell culture incubator to solidify the Matrigel mixture. Next, 100 μL of pig intestinal organoid culture medium was added to each well, and medium composition was as follows: advanced DMEM/F12 supplemented with 1x N2 supplement (Thermo Fisher Scientific), 1x B27 supplement (Thermo Fisher Scientific), 2 mM GlutaMAX™ Supplement (Thermo Fisher Scientific), 10 mM nicotinamide (Sigma-Aldrich), 1 mM N-acetylcysteine (Sigma-Aldrich, St. Louis, MO), 10 mM HEPES (Thermo Fisher Scientific), 100 μg/mL Primocin™ (InvivoGen, San Diego, CA, USA), 50 ng/mL recombinant murine EGF (PMG8041, Thermo Fisher Scientific), 100 ng/mL recombinant murine Noggin (250-38, Peprotech, NJ, USA), 10% R-spondin 1 conditioned media, 50% Wnt-3a conditioned media, 10 μM SB 202190 (Sigma-Aldrich), 0.5 μM A 83-01 (Sigma-Aldrich), 2.5 μM CHIR99021 (Sigma-Aldrich), and 10 μM Y-27632 (Selleckhem, Houston, TX, USA). Pig organoids were cultured for 4 days, and the medium was replaced on day 2. To prevent anoikis in pig organoids, Y-27632 was added for the first two days only.

To maintain pig organoids and develop 2D monolayer organoid, 4-day-cultured organoids were sub-cultured. Matrigel was dissociated using cell recovery solution (Corning Inc.) at 4 °C for 30 min using an orbital shaker with

slow shaking (60 rpm). The organoid-containing supernatant was collected and centrifuged at 200 × *g* for 5 min. Pig organoid pellets were resuspended in advanced DMEM/F12 and physically pipetted. Organoid fragments were counted and cultured on a new plate using the methods described above.

Development of 2D pig intestinal organoids

Sub-cultured organoid fragments were seeded into a 96-well cell culture plate at 12.5 crypts/μL concentration (total volume: 4 μL) and cultured for 2 days. Short-cultured pig organoids were passaged for the sub-culture method, and organoid pellets were incubated with TrypLE Express Enzyme solution (Thermo Fisher Scientific) with occasional pipetting for 10 min in a cell culture incubator. Pig organoids dissociated into single cells were centrifuged at 800 × *g* for 5 min and counted. The single cells were resuspended in 2D pig intestinal organoid culture medium with 20% (v/v) fetal bovine serum added to the pig intestinal organoid culture medium, and seeded at 150,000 cells/cm^2 in pre-coated plates. The pre-coating process was carried out by incubating 2% (v/v) Matrigel with advanced DMEM/F12 medium (50 μL for 96-well cell culture plate) for 1 h in a cell culture incubator. Before single cell seeding, the coating solution was removed and the cells were washed once with advanced DMEM/F12.

Quantitative real-time polymerase chain reaction (qRT-PCR) assay

Total RNA of all samples, including IPEC-J2 cells, 3D organoids, and 2D organoids, was extracted using TRIzol™ Reagent (Thermo Fisher Scientific). The 0.5 μg of RNA was used for cDNA synthesis using the AccuPower® RT PreMix (Bioneer, Daejeon, Korea). qRT-PCR was performed using a QuantStudio 1 Real-Time PCR system (Applied Biosystems, Waltham, CA, USA) and the following conditions were used: 50 °C for 2 min, 95 °C for 15 min, 95 °C for 20 s, and 60 °C for 40 s (40 cycles), followed by melting curve analysis. *GAPDH* was used for normalization of relative gene expression, and the expression level was calculated using the $2^{-\Delta C_T}$ method [21]. The primer sequences for the target genes used in this study are presented in Table 1.

Imaging and immunofluorescent staining

Inverted and confocal microscopes were used to obtain organoid images. A Nikon Eclipse Ts2R microscope (Nikon, Tokyo, Japan) was used to obtain day-to-day 3D and 2D organoid images. Immunofluorescent staining was performed to compare the expression of intestinal epithelial cell markers in IPEC-J2 cells and 3D organoids, and images were obtained using a confocal microscope. Briefly, the cells were fixed in 2% paraformaldehyde

(Biosesang Inc., Gyeonggi-do, Korea) for 30 min at room temperature. After washing with PBS, cells were permeabilized with 1% Triton X-100 (Biosesang Inc.) for 30 min at room temperature. The samples were washed with PBS and blocked with a blocking buffer (10% goat serum and 0.5% Triton X-100) overnight at room temperature. The primary antibodies rabbit anti-Muc2 (27675-1-AP, ProteinTech, IL, USA) and mouse anti-ChgA (sc-393941, Sant Cruz Biotechnology, TX, USA) were diluted at 1:50 and 1:100, respectively, with the blocking buffer. The samples were then incubated for 4 h at room temperature and washed 5 times using the blocking buffer. After washing step, the secondary antibodies, goat anti-rabbit IgG Alexa Fluor 488 (A-11034, Thermo Fisher Scientific) for Muc2 and goat anti-mouse Alexa Fluor 488 for ChgA (A-11029, Thermo Fisher Scientific), were diluted at 1:500 using the blocking buffer. The samples were incubated for 1 h at room temperature in the dark and washed 10 times using the blocking buffer. The samples were stained with Alexa Fluor 555 phalloidin (Thermo Fisher Scientific) (1:200 diluted in PBS) and Hoechst 33342 (Thermo Fisher Scientific) (1:500 diluted in PBS). Both staining processes were performed sequentially, and the samples were incubated in the dark for 30 min at room temperature and washed with PBS. After staining, IPEC-J2 cells and 3D organoids were subjected to confocal microscopy (K1-Fluo; Nanoscope Systems, Daejeon, Korea).

Fatty acid absorption by pig intestinal organoids

To assay fatty acid uptake, C1-BODIPY-C12 (Thermo Fisher Scientific) was used on 3D and 2D organoids, with minor modifications [20]. For the 3D organoid assay, Matrigel was solubilized in a cell recovery solution using the above method. They were resuspended in a solution of 1 μM C1-BODIPY-C12 with 10% fatty acid-free bovine serum albumin solution and incubated in an ultra-low attachment 24-well cell culture plate (Corning Inc., Corning) for 30 min in a cell culture incubator. For the 2D organoid assay, the medium was removed, and they were incubated for 30 min in a cell culture incubator with the same BODIPY solution. The 3D and 2D organoids were fixed in 2% paraformaldehyde and stained with Hoechst 33342 for image analysis. The intracellular fluorescent signal (fluorescent size and intensity) was quantified using NIS-Elements Basic Research software (Nikon).

Lipid mixture (LM) treatment on pig intestinal organoids

The LM (Sigma-Aldrich) was used to treat both 3D and 2D organoids. It contains non-animal derived fatty acids (2 μg/ml arachidonic acid and 10 μg/ml each linoleic, linolenic, myristic, oleic, palmitic, and stearic acids), 0.22 mg/ml cholesterol from New Zealand sheep′s wool, 2.2 mg/ml Tween-80, 70 μg/ml tocopherol acetate, and

100 mg/ml Pluronic F-68 solubilized in cell culture water. Before harvesting the 3D and 2D organoid samples (on day 4 for 3D organoids and on day 2 for 2D organoids), they were treated with 2% LM (v/v) (in each organoid culture medium) for 12-hours. All LM-related organoid experiments, including qRT-PCR, MitoTracker staining, and ADP:ATP ratio assays, were performed using the same method.

Mitochondria staining of pig intestinal organoids

To stain the mitochondria of organoids, MitoTracker™ Green FM (Thermo Fisher Scientific) was used. MitoTracker was prepared as a 1 mM stock in dimethyl sulfoxide according to the manufacturer's instructions. The 3D and 2D organoids were washed once with advanced DMEM/F12, and MitoTracker (final concentration of 100 nM) and Hoechst 33342 (final 1:500 dilution) were added to each organoid culture medium. They were then incubated for 30 min in a cell culture incubator and washed once with advanced DMEM/F12. The stained images were immediately obtained using a confocal microscope.

ADP:ATP ratio assay of pig intestinal organoids

ADP:ATP ratios of 3D and 2D organoids were analyzed according to the bioluminescence method using a SpectraMax iD5 microplate reader (Molecular Devices, San Jose, CA, USA). The assay was conducted using a commercial ADP:ATP Ratio Assay Kit (Abcam, Cambridge, MA, USA) according to the manufacturer's instructions. Briefly, Matrigel was removed from 3D organoids using a cell recovery solution, and single cells were obtained using the TrypLE Express Enzyme solution. After centrifugation, incubation was performed at room temperature for 5 min using the Nucleotide Releasing Buffer of the kit (200 μL per well in a 96-well plate). 2D organoids were washed once with plain advanced DMEM/F12 and incubated at room temperature for 5 min in an equal volume of Nucleotide Releasing Buffer. The remainder of the assay was performed according to the method recommended in the kit using a white 96-well plate (SPL Life Sciences).

Statistical analysis

The experimental data from three to five independent experiments were pooled and presented as mean ± standard deviation. For fatty acid absorption assay, five representative organoid images (3D organoids) and five position images (2D organoids) were randomly selected within each three independent experiments, and fluorescence area and intensity were measured within selected images (average 4.6 and 9.6 fluorescence signal areas for 3D and 2D

organoids, respectively). To determine whether the data were normally distributed, the Shapiro–Wilk test was performed using Prism 8 software (GraphPad, La Jolla, CA, USA). Abnormally distributed data were further analyzed using a two-tailed Mann–Whitney test, and normally distributed data were further analyzed using a two-tailed unpaired *t*-test. The significant difference between groups was considered at $p < 0.05$, and the tendency was considered at $0.05 < p < 0.10$.

Results

Comparison between the IPEC-J2 cell line and 3D pig organoids

First, the characteristics of the IPEC-J2 cell line, a well-known in vitro pig epithelial cell platform, and pig small intestinal 3D organoids were compared. To determine the presence of several types of epithelial cells, mRNA expression levels of epithelial cell marker genes (*LGR5* for crypt-base columnar cells, *LYZ* for Panth cells, *MUC2* for goblet cells, *CHGA* for enteroendocrine cells, and *ALPI* for enterocytes) were compared. In 3D pig organoids, *LYZ* and *ALPI* showed significantly higher gene expression than IPEJ-J2 cells. In addition, *MUC2* and *CHGA* were expressed in 3D pig organoids, but not in the IPEC-J2 cell line (Fig. 1A). *LGR5* was similarly expressed in the organoids and IPEC-J2 cells. Immunofluorescence staining confirmed the presence of MUC2 and CHGA at the protein level. MUC2 and CHGA expressions were observed in 3D pig organoids, but not in IPEC-J2 cells (Fig. 1B and C). These data suggest that pig epithelial cell lines have limitations as in vitro research platforms for studying pig epithelial cells.

Comparison of the gene expression of intestinal epithelial cell markers between 3D and 2D pig organoids

Organoids are normally cultured 3D condition, making it difficult to reproduce phenomenon occurring in the intestinal lumen. As most nutrition-related phenomena occur in the intestinal lumen, a 2D monolayer pig organoid model that can expose the apical membrane was developed in this study. The 3D organoids were fully grown by day 4 by culturing approximately 20 sub-cultured organoid fragments. 2D organoids were seeded with approximately 50,000 single cells from sub-cultured 3D organoids and showed more than 90% confluence on day 2 (Fig. 2A). To compare the expression levels of intestinal epithelial cell marker genes in two fully developed organoids, qRT-PCR was conducted using epithelial cell marker genes. There were no significant differences in *LGR5*, *LYZ*, and *MUC2* between 3D and 2D organoids. However, 2D organoids had significantly higher expression of *CHGA* and *ALPI* than

3D organoids (Fig. 2B). Collectively, these results suggest that, in addition to the structural properties of the 2D organoid model, intestinal epithelial cell marker gene expression differs from that of 3D organoids.

Comparison of nutritional physiology-related factors in different pig organoid models

Because high expression of *CHGA* and *ALPI*, which are important for nutritional physiological responses, was observed in the 2D organoid platform, nutritional function-related gene expression was further compared. To characterize the nutrition-related functions of pig 2D intestinal organoids, the gene expression levels of small intestinal nutrient transporters, gastrointestinal hormones, and brush border enzymes were compared with those in 3D organoids. Except for *GLUT5*, a fructose transporter, most nutrient transporters (*SGLT1*: sodium/glucose transporter, *GLUT2*: glucose transporter, *PEPT1*: peptide transporter, and *CD36*: fatty acid transporter) showed higher gene expression levels in 2D organoids than in 3D organoids (Fig. 3A). Gastrointestinal hormones are mainly secreted by enteroendocrine cells and these hormones are classified into families based on structural homology [22, 23]. In this study, the gastrin family (*GAST* and *CCK*), secretin family (*GCG* and *GIP*), somatostatin family (*SST*), motilin-ghrelin family (*MLN* and *GHRL*), and PP-fold family (*PYY*) were investigated. Among the various hormone-encoding genes, *GCG* was not significantly different between 3D and 2D organoids. However, the expression of other hormone-related genes examined in this study was significantly higher in 2D organoids than in 3D organoids (Fig. 3B). The gene expression of brush border enzymes secreted by enterocytes was compared between the two types of pig organoids. The carbohydrate-related (*SI*, *MGAM*, and *LCT*) and peptide-related (*DPEP1* and *ANPEP*) enzyme genes were significantly highly expressed or tended on 2D organoids than in 3D organoids (Fig. 3C). Collectively, these results suggest that 2D organoids have higher functional gene expression for nutritional physiological responses.

Assessment of nutrient absorption in the different types of pig organoid models

To assess nutrient uptake in 3D and 2D pig intestinal organoids, we used fatty acids as one of the nutrients absorbed by the pig small intestine. To compare the efficiency of fatty acid uptake in each pig organoid model, 3D and 2D organoids were treated with fluorescent fatty acids (Fig. 4A). On average, more lipid droplets were present in 2D organoid images than in 3D organoids. Consistent with this, a larger fluorescence area and brighter fluorescence intensity were observed in 2D organoids than in 3D organoids (Fig. 4B). These data suggest that 2D pig organoids uptake nutrients more efficiently than 3D organoids.

Changes in the expression of nutrient physiology-related factors in pig organoid models after nutrient exposure

Nutrients are absorbed by intestinal epithelial cells, and nutritional physiological phenomena occur through specific receptors and binding proteins. To evaluate the influence of nutrients, especially fatty acids, LM containing various long-chain fatty acids (LCFAs) was treated to 3D and 2D organoids, and selected LCFA-responsive gene expression was investigated. There was no difference in the gene expression of fatty acid-related receptors (*FFAR1* and *FFAR4*) and binding proteins (*FABP1*, *FABP2*, and *FABP5*), which are associated with enteroendocrine cells and enterocytes, in 3D organoids. However, in 2D organoids, a significant increase and increase tendency in the gene expression of *FFAR1* and *FFAR4* was observed after LM treatment (Fig. 5A and B).

Nutrients present in the intestinal lumen or absorbed by enterocytes may act on enteroendocrine cells to regulate gastrointestinal hormone secretion. Some hormones secreted by the small intestine respond to fatty acids. In this study, major fatty acid-responsive hormone genes, such as *GCG*, *CCK*, *GIP*, and *PYY* were examined after LM exposure (Fig. 5C and D). Treatment of 3D organoids with LM showed no difference in hormone genes, but significant increases in the expression of hormone genes other than *GIP* were observed in 2D organoids. Overall, these results indicate that the pig 2D organoid model can mimic the nutrient-induced responses occurring in small intestinal epithelial cells, and that 2D organoids are more responsive to lipid molecules than 3D organoids.

Nutrient metabolism in pig organoid models

Fatty acids absorbed by intestinal epithelial cells are oxidized by mitochondrial activity to produce energy via ATP synthesis. To assess fatty acid-induced mitochondrial activity and ATP patterns in organoids, we confirmed the mitochondria mass and ADP:ATP ratio in LM-treated 3D and 2D organoids. When the two types of organoids were compared using MitoTracker staining, there was no difference in fluorescence intensity between the control and LM groups of 3D organoids. However, in 2D organoids, strong fluorescence intensity was observed in the LM group compared with that in the control group (Fig. 6A). Next, the intracellular ADP:ATP ratios of 3D and 2D pig intestinal organoids were measured. There was no significant difference between the control and LM groups in 3D organoids. However, in 2D organoids, the ADP:ATP ratio was significantly reduced by LM treatment (Fig. 6B). These results indicate that the 2D organoid model has a more active metabolic response to fatty acids, such as the conversion of ADP to ATP, than the 3D organoid model.

Discussion

The gut is a specialized tissue with multiple functions that interacts with the external environment. The epithelial cell layer of the gut plays an important role in the first physical barrier and immune function against harmful external factors, such as pathogens, viruses, and toxins [24]. The small intestine, a part of the gut, consists of various epithelial cell types. The major cell types include crypt-resident stem cells, Paneth cells, goblet cells, enteroendocrine cells, and enterocytes [25]. Intestinal epithelial cells are continuously regenerated at short intervals, and this phenomenon is due to stem cells differentiating into various cell types through progenitor cells [26]. For regulation of intestinal epithelial cells, the function of intestinal stem cells plays a key role, and the LGR5+ cell in the crypt-base has been considered the sole intestinal stem cell marker, but a recent study has reported that various epithelial cells of the isthmus region beyond the crypt also have a stemness potential and are involved in intestinal epithelial cell homeostasis [27]. Therefore, studies related to interactions between multiple cell types are needed to understand the mechanisms of action of complex intestinal epithelial cells. Several cell lines can be used as in vitro platforms to study the responses of intestinal epithelial cells. The inflammatory response regulatory function of short-chain fatty acids, including acetate, propionate, and butyrate, was evaluated in Caco-2 cells, a widely used human intestinal epithelial cell line [28]. Caco-2 cells were treated with 5-Fluorouracil, which is used as a chemotherapy drug for cancer, but caused intestinal mucositis as a side effect, to induce intestinal inflammation. Yue et al. reported that three kinds of short-chain fatty acids inhibit the activation of NLRP3 inflammatory bodies (caspase-1, IL-1β, and IL-18) and increase the expression of gut barrier integrity indicators (Occludin and MUC2) compared with inflammation-induced Caco-2 cells. The use of two human enteroendocrine cell lines, NCL-h716 and HuTu-80, has been reported in studies related to hormone responses, another epithelial cell function [29]. Larraufie et al. reported that short-chain fatty acids (especially propionate and butyrate) strongly regulate hormone production in vitro. The use of epithelial cell lines as an in vitro platform has advantages, such as high reproducibility and economic efficiency. Available epithelial cell lines from domestic animals are very limited thus, the most of domestic animal epithelial cell studies done by using IPEC-J2. For example, probiotic *L. reuteri*, which is isolated from healthy piglet, modulated intestinal health-related factors in LPS-challenged IPEC-J2 cells [30]. Under the challenge conditions, the expression of inflammatory cytokines (TNF-α and IL-6) increased and the expression of tight junction proteins (Claudin-1, Occludin, and ZO-1) expression decreased. However, the above indicators were restored to normal levels through treatment of *L. reuteri* culture supernatant to IPEC-JC2 cells.

However, there are some limitations to using these cell lines in in vitro assays. For example, because most intestinal epithelial cell lines have only a few epithelial cell types, it is difficult to reproduce the epithelial cell combination of complex gut tissues. In addition, immortalization is required to make a stable cell line that can affect the biological function of cell types [31]. Therefore, a better in vitro platform is essential to understand the function of intestinal epithelial cells, and for this reason, intestinal organoids have recently attracted attention [32, 33].

Intestinal organoids have also been established in domestic animals and their applications have been reported in various studies, including physiological gut function, immunity, and nutrition [34, 35]. For example, pig organoids have been used to investigate the mechanism by which deoxynivalenol, a major mycotoxin, inhibits gut epithelial cell development [36]. Deoxynivalenol does not affect the formation efficiency of organoids, but it reduces the differentiation efficiency of organoids and proliferation of epithelial cells by suppressing the Wnt/β-catenin pathway. Domestic animal intestinal organoids can also be used to evaluate immunomodulatory effects of feed additives. A recent study on the immune response to feed additives containing organic acids and essential oils in *S. enterica* challenged chicken organoid model was reported [37]. Treatment with feed additives reduced the bacterial load on organoids and downregulated inflammatory responses by decreasing the gene expression of cytokines and chemokines associated with innate immunity. For intestinal epithelial cell studies, the IPEC-J2 cell line, which is isolated from the neonatal piglet mid-jejunum and is not transformed, has been used in various research fields and has provided important insights into dynamic gut physiology [38]. Although the IPEC-J2 cell line is a useful tool for investigating pig intestines, it has several limitations. For example, unlike other epithelial cell lines, IPEC-J2 cells present a high level of transepithelial resistance, a key parameter of epithelial tightness that affects intracellular processes [39, 40]. Additionally, a comparison of IPEC-J2 cells and actual pig jejunum tissue under common culture conditions (using fetal bovine serum) revealed differences in ion transport properties and cell morphology [38]. Recently, a transcriptome analysis of IPEC-J2 cells, jejunal organoid, and primary gut tissue was reported [41]. A comparison of gene profiling specifically expressed in pig small intestine with primary tissue and in vitro systems showed a pattern of gene expression similar to that of primary tissue in jejunal organoids rather than IPEC-J2 cells. In addition, there was a clear difference in epithelial cell type marker gene expression between the gut tissue and the IPEC-J2 cell line, and the degree of intestinal epithelial cell marker gene expression in primary gut tissue in organoids was similar. The results of this study suggest that it may be more realistic to use organoid models than cell line-based in vitro platforms to study intestinal epithelial cell regulation in pigs. In our study, MUC2 (for goblet cells) and CHGA (for enteroendocrine cells) were compared based on gene and protein expression level (by

immunofluorescence), and it was confirmed that they were not expressed in IPEC-J2 cells but expressed in intestinal organoids. In addition, *LYZ* (for Paneth cells) and *ALPI* (for enterocytes) were highly expressed in pig intestinal organoids compared with IPEC-J2 cells. Our data suggested that 3D organoids are better in vitro systems as they have essential epithelial cell types compared with IPEC-J2 cells. In future studies, comparative research on the functions of epithelial cells should be conducted to determine the advantages of pig intestinal organoids.

The intestine has various physiological functions, such as immune regulation, physical barriers to harmful external materials, and nutrient absorption [25]. Nutrient absorption is mainly mediated by enteroendocrine cells and enterocytes in intestinal epithelial cells. Enteroendocrine cells and enterocytes are more directly related to nutrition than other epithelial cell types. Enteroendocrine cells are distributed throughout the epithelium of the gastrointestinal tract, including the small intestine. They release several gut hormones in response to food intake and control gut motility or other endocrinal response [42]. Enterocytes are the major cells responsible for nutrient absorption and are the highest proportion of epithelial cell types [43]. Dietary food delivered to the intestine lumen is broken down into small units of nutrients by digestive enzymes that are sensed by enteroendocrine cells or enterocytes. Enteroendocrine cells secrete gastrointestinal hormones that regulate various organ systems, and enterocytes directly absorb small nutrients [44]. A sequential process involving intestinal digestive enzymes, nutrient-specific transporters, and hormone secretion is required for this series of nutrient-related processes. The intestinal organoid system has three characteristic factors and functional response of nutrient use [17, 45]. For example, there was a difference in the degree of nutrient absorption when nutrient-related transporters were treated with transporter inhibitors or transporter gene knock-out organoids, and there was also a difference in the levels of secreted hormones in hormone gene knock-out organoids [45]. These results suggest that the gut organoids play a functional role in nutrient processing. However, there is no clear information regarding the nutrient process-related functions of 3D organoids compared with those of IPEC-J2 cells. In our study, we found that 3D organoids differed in the expression of *CHGA* and *ALPI* associated with the nutrient process compared with the IPEC-J2 cell line (*CHGA*: expressed only in 3D organoids; *ALPI*: higher gene expression in 3D organoids). Some nutrient process-related gene expression also showed similar differences between 3D organoids and the IPEC-J2 cell line (Fig. S1).

Although organoid systems have several advantages, they have structural limitations related to the physical properties of the intestine. The apical side of epithelial cells, which are in contact with the lumen of the intestine and consist of microvilli, performs various biological functions, such as mucus secretion, gut microbiota sensing, and

nutrient processing [46]. 3D intestinal organoids, a general culture method, are not exposed to the outside of the intestinal lumen; therefore, some studies require advanced techniques such as microinjection [47, 48]. Owing to the 3D organoid structure, several organoid culture models have been reported to modify the 3D culture method according to the purpose of the study [20, 49-51]. For example, when comparing physical indicators, such as permeability measurements, the structure of organoids affects the outcome of study. Some receptors that regulate the physical function of intestinal epithelium exist in the apical membrane of epithelial cells. Thus, 3D organoid may not suitable model to understand regulatory response of gut permeability induced by receptors [52]. In this study, we developed a pig 2D organoid model and compared it with a pig 3D organoid model, focusing on nutritional perspectives. Surprisingly, the 2D organoid model had *CHGA* and *ALPI*, which are related to nutrient processing, and when fully developed, their expression levels are significantly higher than those of the 3D organoid model. Furthermore, the expression of most nutrient transporter genes was higher in 2D pig organoids. In line with this, many gastrointestinal hormones and digestive enzyme genes were highly expressed on the pig 2D organoid model. These results suggest that pig 2D intestinal organoid models not only have structural and characteristic advantages in nutrition-related studies, but also have superior potential for nutritional physiological responses.

As gene expression levels have limited information, we further attempted to confirm the functional activity of nutrient processing and related response by comparing 3D and 2D pig organoids. We compared the nutrient absorption of two pig organoid models using a fluorescent fatty acid analog. Fluorescent-conjugated nutrients are widely used in studies of nutrient uptake in organoids for intestinal function research [53, 54]. Basic organoid cultures have an apical membrane formed inward, similar to the actual intestinal shape, and these structures may affect uptake in the intestinal lumen. Therefore, studies on physiological phenomena such as nutrient uptake and drug absorption have reported changes in the culture methods of intestinal organoids [54, 55]. In previous study, differences in nutrient uptake according to organoid culture method have been reported [56]. An apical-out culture method, which exposed the apical side of the intestinal epithelium that absorbs nutrients from the outside, absorbed more nutrients (including fatty acid, amino acid, and glucose) than organoids of the conventional method. Thus, structural property of organoid models should be considered for conducting nutritional study. Compared with the pig 3D organoid model, we found that the pig 2D organoid model absorbed more fatty acids during the same period. Although the exposed apical membrane of the 2D intestinal organoid model facilitate the absorption of fatty acids, nutrients can be diffused or actively transported depending on their type, and the degree of uptake can vary

406 depending on the location of nutrient transporters (basal, apical, or both) [57]. Therefore, suitable culture models for
407 target nutrients should be considered in future organoid-based nutritional studies.

408 Fatty acids, one of the major nutrients, are broken down from dietary lipids in the intestine and absorbed mainly
409 by enterocytes. Fatty acid metabolism involves several proteins including receptors, transporters, and binding
410 proteins [58]. Unlike other nutrients, fatty acid absorption pathways exhibit unique properties. First, fatty acids are
411 re-esterified by related complex molecules before entering enterocytes through the apical membrane. The absorbed
412 fatty acids are then packaged into pre-chylomicrons or stored as intracellular lipid droplets for fatty acid oxidation.
413 Finally, mature chylomicrons are released from the enterocytes and transported throughout the body via the
414 lymphatic system [59]. Nutrients can induce various signals in the gastrointestinal tract, including peptide hormone
415 release by enteroendocrine cells. These hormones act efficiently over the short term and are secreted by several
416 types of enteroendocrine cells that secrete hormones such as glucagon-like peptide 1 and 2 (GLP-1 and GLP-2),
417 cholecystokinin (CCK), glucose-dependent insulinotropic polypeptide (GIP), and peptide YY (PYY) [42]. As an
418 example of hormone release by fatty acids, it has been reported that LCFAs significantly induce the release of GLP-
419 1 and GLP-2 in the pig gut tissue ex vivo culture model [60]. To confirm the response to fatty acids, especially
420 LCFAs, in pig intestinal organoid models, we compared the gene expression levels of fatty acid metabolism-related
421 proteins and hormones after treatment with LM. In summary, no significant differences were found in the 3D
422 organoid model; however, in the 2D organoid model, the LCFA receptor and several hormone-encoding genes
423 showed an overall increase after LM treatment. FFAR1 and FFAR4 (as well-known GPR 40 and GPR120,
424 respectively) are representative LCFA receptors as types of G protein-coupled receptor (GPCR). And they that are
425 expressed in several enteroendocrine cell types and are associated with hormones [61]. Some gut hormones,
426 including CCK, GLP-1, and PYY, are well known for their anorexic activity, in which their concentrations rise soon
427 after food ingestion and remain elevated for up to several hours, depending on meal size and composition [62]. Lipid
428 intake in food stimulates the release of these hormones and increases their plasma concentrations [63, 64]. To
429 support the association between receptors and hormones, deficient mouse models of FFAR1 or FFAR4 have been
430 shown to impair lipid-induced hormone secretion responses [65, 66]. Our 2D pig intestinal organoid model
431 suggested that fatty acids can be recognized by receptors in the apical membrane and can simulate hormonal
432 responses similar to those in the intestinal lumen. However, since there are limitations due to comparisons at the
433 genetic level, it is necessary to directly compare hormone secretion levels or study the mechanism of the
434 intracellular fatty acid-induced pathway up to hormone release.

LCFAs can be divided into saturated and unsaturated fatty acids based on their 12–20 carbon chain composition. LCFAs absorbed by cells are regulated by several metabolic responses, including cellular metabolism, energy homeostasis, and cell proliferation [67]. Various LCFAs, like other nutrients, can diffuse or be transferred through specific proteins. First, LCFAs uptake is carried out by plasma membrane-associated fatty acid-binding protein (FABPpm) such as fatty acid transport protein 4 (FATP4), and cluster of differentiation 36 (CD36) in enterocytes. LCFAs absorbed by acyl-CoA synthetase (ASC) are present as free fatty acids or fatty acyl coenzyme A (fatty acyl-CoA). They are then bound by fatty acid-binding protein (FABP) and acyl-CoA binding protein (ACBP) and trafficked into the cells [68]. Fatty acyl-CoA migrates to the mitochondria, and intramitochondrial oxidation proceeds via the beta oxidation pathway. The mitochondrial matrix does not contain enzymes that activate fatty acids containing 14 or more carbon atoms. Thus, the entry of LCFAs into the mitochondria is regulated by specific enzyme activities, such as carnitine palmitoyltransferase 1 (CPT 1) and CPT 2. Acetyl coenzyme A (acetyl-CoA) is produced as an end product of beta oxidation, and it promotes ATP synthesis through the tricarboxylic acid (TCA) cycle [69]. To confirm LCFAs-induced metabolism in pig organoid models, mitochondria staining and intracellular ADP:ATP ratios were compared. In our study, LM treatment increased mitochondrial fluorescence intensity in 2D organoids but not in 3D organoids. In addition, there was no significant difference in the ADP:ATP ratio after LM treatment in 3D organoids, whereas it decreased in 2D organoids. The ADP:ATP ratio reduction may imply the presence of a larger proportion of ATP within the cells, which, together with the mitochondria staining results, may have contributed to the generation of ATP through fatty acid oxidation within the 2D organoids. However, no changes were observed in 3D organoids, which may have caused poor fatty acid transfer into the cells or differences in fatty acid oxidation-related enzyme activity. Collectively, 2D and 3D organoid systems show different physiological response in nutrient metabolism maybe due to poor nutrient absorption and/or lower expression of nutrient process-related cells and gene expression.

Conclusion

In summary, our results suggested that pig intestinal organoids are more suitable for intestinal epithelial cell research than the existing in vitro systems such as IPEC-J2. Furthermore, we have established a 2D organoid model for intestinal lumen research and further compared nutrient-related properties, such as nutrient transporters, hormones, and digestive enzymes, with a 3D organoid model to characterize them. Compared with the 3D organoid model, the established 2D organoid model showed more active absorption of nutrients, gene expression, and metabolic

processes related to nutrient responses. These findings emphasize the suitability of the 2D organoid model as an in vitro platform for nutrition-related research and provide an improved understanding of nutrient use by intestinal epithelial cells. This study provides essential information for further investigations of the interactions between intestinal epithelial cells and nutrients in the gut environment.

Acknowledgments

Not applicable.

References

1. Maes DG, Dewulf J, Piñeiro C, Edwards S, Kyriazakis I. A critical reflection on intensive pork production with an emphasis on animal health and welfare. J Anim Sci. 2020;98(Supplement_1):S15-S26. https://doi.org/10.1093/jas/skz362
2. Kim KY, Ko HJ, Kim HT, Kim CN, Byeon SH. Association between pig activity and environmental factors in pig confinement buildings. Aust J Exp Agric. 2008;48(5):680-6. https://doi.org/10.1071/EA06110
3. Rutherford K, Baxter E, D'eath R, Turner S, Arnott G, Roehe R, et al. The welfare implications of large litter size in the domestic pig I: biological factors. Anim Welf. 2013;22(2):199-218. https://doi.org/10.7120/09627286.22.2.199
4. Lallès JP, Bosi P, Smidt H, Stokes CR. Nutritional management of gut health in pigs around weaning. Proc Nutr Soc. 2007;66(2):260-8. https://doi.org/10.1017/S0029665107005484
5. Che L, Zhou Q, Liu Y, Hu L, Peng X, Wu C, et al. Flaxseed oil supplementation improves intestinal function and immunity, associated with altered intestinal microbiome and fatty acid profile in pigs with intrauterine growth retardation. Food Funct. 2019;10(12):8149-60. https://doi.org/10.1039/C9FO01877H
6. Saleri R, Borghetti P, Ravanetti F, Cavalli V, Ferrari L, De Angelis E, et al. Effects of different short-chain fatty acids (SCFA) on gene expression of proteins involved in barrier function in IPEC-J2. Porcine Health Manag. 2022;8(1):21. https://doi.org/10.1186/s40813-022-00264-z
7. Du Y, Li X, Niu Q, Mo X, Qui M, Ma T, et al. Development of a miniaturized 3D organoid culture platform for ultra-high-throughput screening. J Mol Cell Biol. 2020;12(8):630-43. https://doi.org/10.1093/jmcb/mjaa036
8. Hou Q, Ye L, Liu H, Huang L, Yang Q, Turner J, et al. Lactobacillus accelerates ISCs regeneration to protect the integrity of intestinal mucosa through activation of STAT3 signaling pathway induced by LPLs secretion of

IL-22. Cell Death Differ. 2018;25(9):1657-70. https://doi.org/10.1038/s41418-018-0070-2

9. Clevers H. Modeling development and disease with organoids. Cell. 2016;165(7):1586-97.
10. Rossi G, Manfrin A, Lutolf MP. Progress and potential in organoid research. Nat Rev Genet. 2018;19(11):671-87. https://doi.org/10.1016/j.cell.2016.05.082
11. Rookmaaker MB, Schutgens F, Verhaar MC, Clevers H. Development and application of human adult stem or progenitor cell organoids. Nature Reviews Nephrology. 2015;11(9):546-54. https://doi.org/10.1038/nrneph.2015.118
12. Kawasaki M, Goyama T, Tachibana Y, Nagao I, Ambrosini YM. Farm and companion animal organoid models in translational research: a powerful tool to bridge the gap between mice and humans. Front Med Technol. 2022;4:895379. https://doi.org/10.3389/fmedt.2022.895379
13. Sato T, Stange DE, Ferrante M, Vries RG, Van Es JH, Van Den Brink S, et al. Long-term expansion of epithelial organoids from human colon, adenoma, adenocarcinoma, and Barrett's epithelium. Gastroenterology. 2011;141(5):1762-72. https://doi.org/10.1053/j.gastro.2011.07.050
14. Blake R, Jensen K, Mabbott N, Hope J, Stevens J. The development of 3D bovine intestinal organoid derived models to investigate Mycobacterium avium ssp paratuberculosis pathogenesis. Front Vet Sci. 2022;9:921160. https://doi.org/10.3389/fvets.2022.921160
15. Smith D, Price DR, Burrells A, Faber MN, Hildersley KA, Chintoan-Uta C, et al. The development of ovine gastric and intestinal organoids for studying ruminant host-pathogen interactions. Front Cell Infect Microbiol. 2021;11:733811. https://doi.org/10.3389/fcimb.2021.733811
16. Li J, Li Jr J, Zhang S, Li R, Lin X, Mi Y, et al. Culture and characterization of chicken small intestinal crypts. Poult Sci. 2018;97(5):1536-43. https://doi.org/10.3382/ps/pey010
17. Gonzalez LM, Williamson I, Piedrahita JA, Blikslager AT, Magness ST. Cell lineage identification and stem cell culture in a porcine model for the study of intestinal epithelial regeneration. PloS One. 2013;8(6):e66465. https://doi.org/10.1371/journal.pone.0066465
18. Derricott H, Luu L, Fong WY, Hartley CS, Johnston LJ, Armstrong SD, et al. Developing a 3D intestinal epithelium model for livestock species. Cell Tissue Res. 2019;375:409-24. https://doi.org/10.1007/s00441-018-2924-9
19. Li Y, Yang N, Chen J, Huang X, Zhang N, Yang S, et al. Next-generation porcine intestinal organoids: an apical-out organoid model for swine enteric virus infection and immune response investigations. J Virol.

2020;94(21):10.1128/jvi. 01006-20. https://doi.org/10.1128/jvi.01006-20

20. Joo SS, Gu BH, Park YJ, Rim CY, Kim MJ, Kim SH, et al. Porcine intestinal apical-out organoid model for gut function study. Animals (Basel). 2022;12(3):372. https://doi.org/10.3390/ani12030372
21. Schmittgen TD, Livak KJ. Analyzing real-time PCR data by the comparative CT method. Nat Protoc. 2008;3(6):1101-8. https://doi.org/10.1038/nprot.2008.73
22. Ahlman H, Nilsson O. The gut as the largest endocrine organ in the body. Ann Oncol. 2001;12:S63-S8. https://doi.org/10.1093/annonc/12.suppl_2.S63
23. Ohno T, Mochiki E, Kuwano H. The roles of motilin and ghrelin in gastrointestinal motility. Int J of Pept. 2010;2010(1):820794. https://doi.org/10.1155/2010/820794
24. Chelakkot C, Ghim J, Ryu SH. Mechanisms regulating intestinal barrier integrity and its pathological implications. Exp Mol Med. 2018;50(8):1-9. https://doi.org/10.1038/s12276-018-0126-x
25. Peterson LW, Artis D. Intestinal epithelial cells: regulators of barrier function and immune homeostasis. Nat Rev Immunol. 2014;14(3):141-53. https://doi.org/10.1038/nri3608
26. De Santa Barbara P, Van Den Brink GR, Roberts DJ. Development and differentiation of the intestinal epithelium. Cell Mol Life Sci. 2003;60:1322-32. https://doi.org/10.1007/s00018-003-2289-3
27. Malagola E, Vasciaveo A, Ochiai Y, Kim W, Zheng B, Zanella L, et al. Isthmus progenitor cells contribute to homeostatic cellular turnover and support regeneration following intestinal injury. Cell. 2024;187(12):3056-71. e17. https://doi.org/10.1016/j.cell.2024.05.004
28. Iglesias DE, Cremonini E, Fraga CG, Oteiza PI. Ellagic acid protects Caco-2 cell monolayers against inflammation-induced permeabilization. Free Radic Biol Med. 2020;152:776-86. https://doi.org/10.1016/j.freeradbiomed.2020.01.022
29. Larraufie P, Martin-Gallausiaux C, Lapaque N, Dore J, Gribble F, Reimann F, et al. SCFAs strongly stimulate PYY production in human enteroendocrine cells. Sci Rep. 2018;8(1):74. https://doi.org/10.1038/s41598-017-18259-0
30. Yang F, Wang A, Zeng X, Hou C, Liu H, Qiao S. Lactobacillus reuteri I5007 modulates tight junction protein expression in IPEC-J2 cells with LPS stimulation and in newborn piglets under normal conditions. BMC microbiol. 2015;15:1-11. https://doi.org/10.1186/s12866-015-0372-1
31. Kaur G, Dufour JM. Cell lines: Valuable tools or useless artifacts. Spermatogenesis. 2012;2(1):1-5. https://doi.org/10.4161/spmg.19885

32. Sato T, Vries RG, Snippert HJ, Van De Wetering M, Barker N, Stange DE, et al. Single Lgr5 stem cells build crypt-villus structures in vitro without a mesenchymal niche. Nature. 2009;459(7244):262-5. https://doi.org/10.1038/nature07935
33. Fujii M, Matano M, Toshimitsu K, Takano A, Mikami Y, Nishikori S, et al. Human intestinal organoids maintain self-renewal capacity and cellular diversity in niche-inspired culture condition. Cell stem cell. 2018;23(6):787-93. e6. https://doi.org/10.1016/j.stem.2018.11.016
34. Yin YB, Guo SG, Wan D, Wu X, Yin YL. Enteroids: promising in vitro models for studies of intestinal physiology and nutrition in farm animals. J Agric Food Chem. 2019;67(9):2421-8. https://doi.org/10.1021/acs.jafc.8b06908
35. Seeger B. Farm animal-derived models of the intestinal epithelium: recent advances and future applications of intestinal organoids. Altern Lab Anim. 2020;48(5-6):215-33. https://doi.org/10.1177/026119292097402
36. Li XG, Zhu M, Chen MX, Fan HB, Fu HL, Zhou JY, et al. Acute exposure to deoxynivalenol inhibits porcine enteroid activity via suppression of the Wnt/β-catenin pathway. Toxicol Lett. 2019;305:19-31. https://doi.org/10.1016/j.toxlet.2019.01.008
37. Mitchell J, Sutton K, Elango JN, Borowska D, Perry F, Lahaye L, et al. Chicken intestinal organoids: a novel method to measure the mode of action of feed additives. Front Immunol. 2024;15:1368545. https://doi.org/10.3389/fimmu.2024.1368545
38. Brosnahan AJ, Brown DR. Porcine IPEC-J2 intestinal epithelial cells in microbiological investigations. Vet Microbiol. 2012;156(3-4):229-37. https://doi.org/10.1016/j.vetmic.2011.10.017
39. Zakrzewski SS, Richter JF, Krug SM, Jebautzke B, Lee IFM, Rieger J, et al. Improved cell line IPEC-J2, characterized as a model for porcine jejunal epithelium. PloS one. 2013;8(11):e79643. https://doi.org/10.1371/journal.pone.0079643
40. Günzel D, Fromm M. Claudins and other tight junction proteins. Compr Physiol. 2012;2(3):1819-52. https://doi.org/10.1002/cphy.c110045
41. Van der Hee B, Madsen O, Vervoort J, Smidt H, Wells JM. Congruence of transcription programs in adult stem cell-derived jejunum organoids and original tissue during long-term culture. Front Cell Dev Biol. 2020;8:529393. https://doi.org/10.3389/fcell.2020.00375
42. Gribble FM, Reimann F. Enteroendocrine cells: chemosensors in the intestinal epithelium. Annu Rev Physiol. 2016;78(1):277-99. https://doi.org/10.1146/annurev-physiol-021115-105439

43. Wang Y, Song W, Wang J, Wang T, Xiong X, Qi Z, et al. Single-cell transcriptome analysis reveals differential nutrient absorption functions in human intestine. J Exp Med. 2020;217(2). https://doi.org/10.1084/jem.20191130
44. McCauley HA. Enteroendocrine regulation of nutrient absorption. J Nutr. 2020;150(1):10-21. https://doi.org/10.1093/jn/nxz191
45. Zietek T, Rath E, Haller D, Daniel H. Intestinal organoids for assessing nutrient transport, sensing and incretin secretion. Sci Rep. 2015;5(1):16831. https://doi.org/10.1038/srep16831
46. Sauvanet C, Wayt J, Pelaseyed T, Bretscher A. Structure, regulation, and functional diversity of microvilli on the apical domain of epithelial cells. Annu Rev Cell Dev Biol. 2015;31(1):593-621. https://doi.org/10.1146/annurev-cellbio-100814-125234
47. Williamson IA, Arnold JW, Samsa LA, Gaynor L, DiSalvo M, Cocchiaro JL, et al. A high-throughput organoid microinjection platform to study gastrointestinal microbiota and luminal physiology. Cell Mol Gastroenterol Hepatol. 2018;6(3):301-19. https://doi.org/10.1016/j.jcmgh.2018.05.004
48. Hill DR, Huang S, Tsai YH, Spence JR, Young VB. Real-time measurement of epithelial barrier permeability in human intestinal organoids. J Vis Exp. 2017(130):e56960. https://doi.org/10.3791/56960
49. Kar SK, Van Der Hee B, Loonen LM, Taverne N, Taverne-Thiele JJ, Schokker D, et al. Effects of undigested protein-rich ingredients on polarised small intestinal organoid monolayers. J Anim Sci Biotechnol. 2020;11:1-7. https://doi.org/10.1186/s40104-020-00443-4
50. Wright CW, Li N, Shaffer L, Hill A, Boyer N, Alves SE, et al. Establishment of a 96-well transwell system using primary human gut organoids to capture multiple quantitative pathway readouts. Sci Rep. 2023;13(1):16357. https://doi.org/10.1038/s41598-023-43656-z
51. Kasendra M, Tovaglieri A, Sontheimer-Phelps A, Jalili-Firoozinezhad S, Bein A, Chalkiadaki A, et al. Development of a primary human Small Intestine-on-a-Chip using biopsy-derived organoids. Sci Rep. 2018;8(1):1-14. https://doi.org/10.1038/s41598-018-21201-7
52. Bardenbacher M, Ruder B, Britzen-Laurent N, Schmid B, Waldner M, Naschberger E, et al. Permeability analyses and three dimensional imaging of interferon gamma-induced barrier disintegration in intestinal organoids. Stem Cell Res. 2019;35:101383. https://doi.org/10.1016/j.scr.2019.101383
53. Margalef-Català M, Li X, Mah AT, Kuo CJ, Monack DM, Amieva MR. Controlling epithelial polarity: a human enteroid model for host-pathogen interactions. Cell Rep. 2019;26(9):2509-20. e4.

https://doi.org/10.1016/j.celrep.2019.01.108

54. Zhang W, Tian Y, Chen B, Xu S, Wu L. PFOA/PFOS Facilitated Intestinal Fatty Acid Absorption by Activating the PPARα Pathway: Insights from Organoids Model. Environ Health (Wash). 2023;2(2):85-94. https://doi.org/10.1021/envhealth.3c00129
55. Li D, Rodia CN, Johnson ZK, Bae M, Muter A, Heussinger AE, et al. Intestinal basolateral lipid substrate transport is linked to chylomicron secretion and is regulated by apoC-III. J Lipid Res. 2019;60(9):1503-15. https://doi.org/10.1194/jlr.M092460
56. Kang TH, Lee SI. Establishment of a chicken intestinal organoid culture system to assess deoxynivalenol-induced damage of the intestinal barrier function. J Anim Sci Biotechnol. 2024;15(1):30. https://doi.org/10.1186/s40104-023-00976-4
57. Duca FA, Waise TZ, Peppler WT, Lam TK. The metabolic impact of small intestinal nutrient sensing. Nat Commun. 2021;12(1):903. https://doi.org/10.1038/s41467-021-21235-y
58. Gajda AM, Storch J. Enterocyte fatty acid-binding proteins (FABPs): different functions of liver and intestinal FABPs in the intestine. Prostaglandins Leukot Essent Fatty Acids. 2015;93:9-16. https://doi.org/10.1016/j.plefa.2014.10.001
59. Ko CW, Qu J, Black DD, Tso P. Regulation of intestinal lipid metabolism: current concepts and relevance to disease. Nat Rev Gastroenterol Hepatol. 2020;17(3):169-83. https://doi.org/10.1038/s41575-019-0250-7
60. Voortman T, Hendriks HF, Witkamp RF, Wortelboer HM. Effects of long-and short-chain fatty acids on the release of gastrointestinal hormones using an ex vivo porcine intestinal tissue model. J Agric Food Chem. 2012;60(36):9035-42. https://doi.org/10.1021/jf2045697
61. Grundmann M, Bender E, Schamberger J, Eitner F. Pharmacology of free fatty acid receptors and their allosteric modulators. Int J Mol Sci. 2021;22(4):1763. https://doi.org/10.3390/ijms22041763
62. Gribble FM, Reimann F. Function and mechanisms of enteroendocrine cells and gut hormones in metabolism. Nat Rev Endocrinol. 2019;15(4):226-37. https://doi.org/10.1038/s41574-019-0168-8
63. Ekberg JH, Hauge M, Kristensen LV, Madsen AN, Engelstoft MS, Husted AS, et al. GPR119, a major enteroendocrine sensor of dietary triglyceride metabolites coacting in synergy with FFA1 (GPR40). Endocrinology. 2016;157(12):4561-9. https://doi.org/10.1210/en.2016-1334
64. Mandøe MJ, Hansen KB, Windeløv JA, Knop FK, Rehfeld JF, Rosenkilde MM, et al. Comparing olive oil and C4-dietary oil, a prodrug for the GPR119 agonist, 2-oleoyl glycerol, less energy intake of the latter is needed to

stimulate incretin hormone secretion in overweight subjects with type 2 diabetes. Nutr Diabetes. 2018;8(1):2. https://doi.org/10.1038/s41387-017-0011-z

65. Iwasaki K, Harada N, Sasaki K, Yamane S, Iida K, Suzuki K, et al. Free fatty acid receptor GPR120 is highly expressed in enteroendocrine K cells of the upper small intestine and has a critical role in GIP secretion after fat ingestion. Endocrinology. 2015;156(3):837-46. https://doi.org/10.1210/en.2014-1653
66. Liou AP, Lu X, Sei Y, Zhao X, Pechhold S, Carrero RJ, et al. The G-protein− coupled receptor GPR40 directly mediates long-chain fatty acid− induced secretion of cholecystokinin. Gastroenterology. 2011;140(3):903-12. e4. https://doi.org/10.1053/j.gastro.2010.10.012
67. He Q, Chen Y, Wang Z, He H, Yu P. Cellular uptake, metabolism and sensing of long-chain fatty acids. Front Biosci (Landmark Ed). 2023;28(1):10. https://doi.org/10.31083/j.fbl2801010
68. Niot I, Poirier H, Tran TTT, Besnard P. Intestinal absorption of long-chain fatty acids: evidence and uncertainties. Prog Lipid Res. 2009;48(2):101-15. https://doi.org/10.1016/j.plipres.2009.01.001
69. Nguyen P, Leray V, Diez M, Serisier S, Bloc'h JL, Siliart B, et al. Liver lipid metabolism. J Anim Physiol Anim Nutr (Berl). 2008;92(3):272-83. https://doi.org/10.1111/j.1439-0396.2007.00752.x

70.

Tables and Figures

Table 1. List of primers in this study

Gene	Description	Forward	Reverse	Size (base pair)
LGR5	Leucine-rich repeat-containing G-protein coupled receptor 5	CCTTGGCCCTGAACAAAATA	ATTTCTTTCCCAGGGAGTGG	110
LYZ	Lysozyme	GCAAGACACCCAAAGCAGTT	ATGCCACCCATGCTTTAACG	132
MUC2	Mucin 2	GCTGGCCGACAACAAGAAGA	TGGTGGGAGGATGGTTGGAA	126
CHGA	Chromogranin-A	TGAAGTGCATCGTCGAGGTC	GAGGATCCGTTCATCTCCTCG	104
ALPI	Alkaline Phosphatase, Intestinal	AGGAACCCAGAGGGACCATTC	CACAGTGGCTGAGGGACTTAGG	83
SGLT1	Sodium/glucose cotransporter 1	GTCGTCTCCCTCTTCACCAAG	ATGGTCTCTTCTGGGGCTTCT	137
GLUT2	Glucose transporter 2	CCAGGCCCCATCCCCTGGTT	GCGGGTCCAGTTGCTGAATGC	96
GLUT5	Glucose transporter 5	CCCAGGAGCCGGTCAAG	TCAGCGTCGCCAAAGCA	60
PEPT1	Peptide transporter 1	TTCTAAGCAGCCAGCCATGAA	CCAGTGTTGTGTGTGTGTGTG	119
CD36	Cluster of differentiation 36	GGAGAAAAGATCACTACCATCATGAG	CTCCTGAAGTGCAATGTACTGACA	78
GAST	Gastrin	TGGATGGAGGAGGAAGAAGAAG	TTGGCTTTCATGTGGCTGGA	142
CCK	Cholecystokinin	CAGGCTCGAAAAGCACCTTC	GCGGGGTCTTCTAGGAGGTA	157
GCG	Proglucagon	AGAACTCCGCCGCAGACA	TAAAGTCTCGGGTGGCAAGATT	83
GIP	Gastric Inhibitory Polypeptide	GGACAAGATCCGCCAACAAGA	CTCGCCTCCTCCTTCCTGTTA	141
SST	Somatostatin	CCCAACCAGACAGAGAACGAT	GGCCGGGTTTGAGTTAGCT	108
MLN	Motilin	CCAGAATGCCGCCAAGTAACA	GCTGTTTGGGAGAGGGTGTTT	124
GHRL	Ghrelin	AAGAAGCCAGCAGCCAAACT	GACTGAGCCCCTGACAACTT	149
PYY	Peptide YY	ACTCCTCTCGCCTTCCATTTC	AGTGTCCCCAGGCAGATGA	127
SI	Sucrase-isomaltase	GGCCATGGAGAAAACAACGT	TCGGCTGGCAGTTGTAGTTA	119
MGAM	Maltase-glucoamylase	TCATCATCTCTCGCTCCACC	GGCTAAACTCCATCATGCCG	120
LCT	Lactase	ACAATGCCACTGGAGACGTA	GAAAACCCGAGACCAGGAGA	119
DPEP1	Dipeptidase 1	GAGCGTCGTGAAGGAGATGAA	CGAGGAGTGGCTGAAGATGAC	121
ANPEP	Alanyl aminopeptidase	ACATCCTACCCACTCCCCAAA	TCGCTCTTTGTTGCTGATGGA	144
FFAR1	Free fatty acid receptor 1	GAGGCTGGCTGGACAATACTA	AGAAGAACAGGAGAGAGAGGC	132
FFAR4	Free fatty acid receptor 4	GCACCCGTGTACCTGCTTTA	AAGGAACCCACAGCAAATCCTTT	127
FABP1	Fatty acid binding protein 1	GGAAGGACATCAAGGGGACAT	AGTCAGGGTCTCCATCTCACA	131
FABP2	Fatty acid binding protein 2	TTAACTACAGCCTCGCAGACG	CCTCTTGGCTTCTACTCCTTCA	176
FABP5	Fatty acid binding protein 5	AGGCACCAGTCCGCTTATTC	GCCATTCCCACTCCTACTTCC	138
GAPDH	Glyceraldehyde-3-phosphate dehydrogenase	ATTCCACCCACGGCAAGTTC	CACCAGCATCACCCCATTTG	126

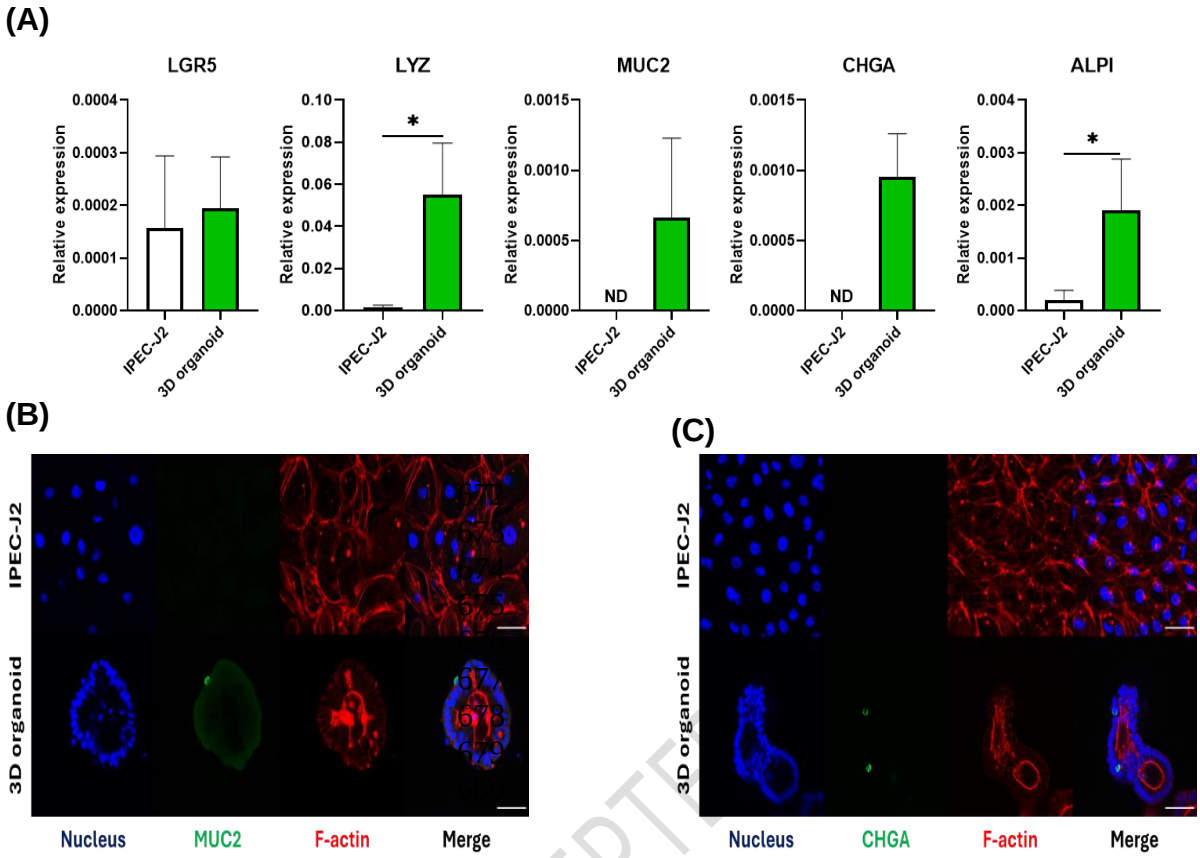

Fig. 1 Comparison of IPEC-J2 cell and pig intestinal organoids. (A**)** Expression of the mRNA levels of epithelial cell marker genes in IPEC-J2 and pig intestinal organoids. Data are presented as mean ± standard deviation (n = 3-5). $^{*}p < 0.05$, ND; non-detected. (B**)** Immunostaining of MUC2 in IPEC-J2 and pig intestinal organoids. (C**)** Immunostaining of CHGA in IPEC-J2 and pig intestinal organoids. Nucleus and F-actin were stained with Hoechst 33342 and phalloidin. Scale bar = 50 μm.

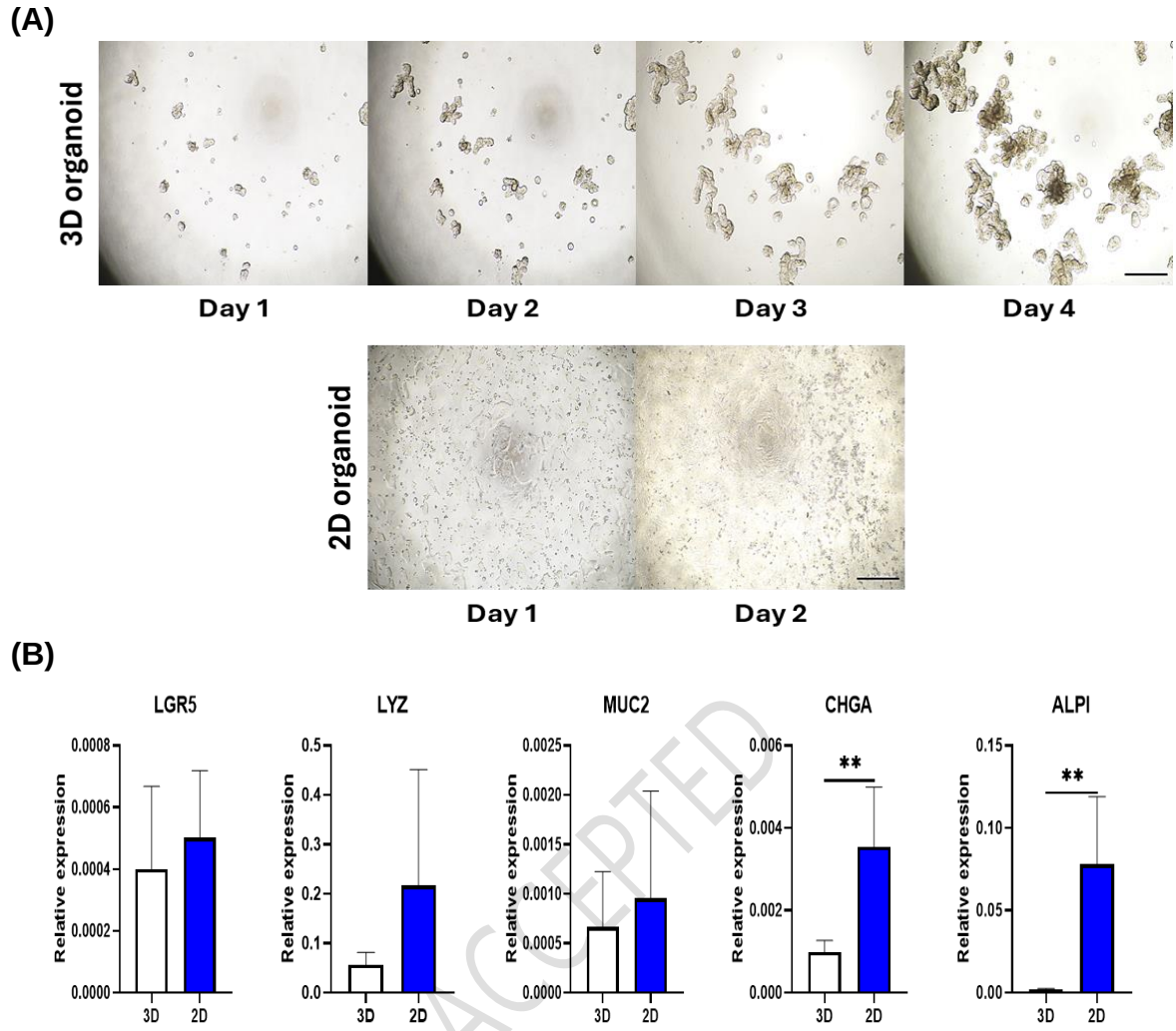

Fig. 2 Development of 2D pig intestinal organoids. (A) Representative image of 3D and 2D pig intestinal organoids. Scale bar = 500 μm. (B) Expression of the mRNA levels of epithelial cell marker genes in 3D and 2D pig intestinal organoids. Data are presented as mean ± standard deviation (n = 5). $^{**}p < 0.01$.

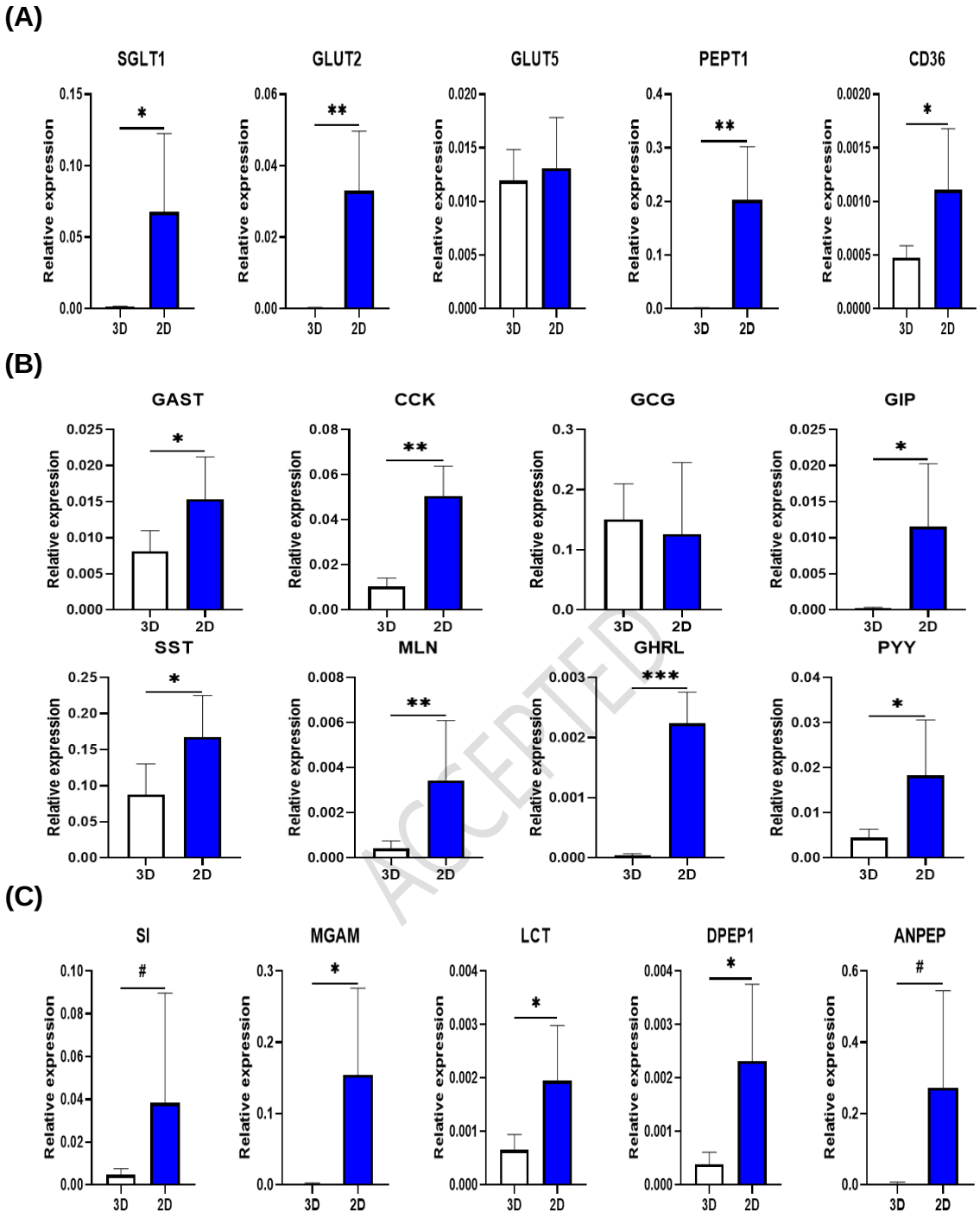

Fig. 3 Nutrition-related properties of 3D and 2D pig intestinal organoids. (A) Expression of the mRNA levels of nutrient transporter genes in 3D and 2D pig intestinal organoids. (B) Expression of the mRNA levels of gastrointestinal hormone genes in 3D and 2D pig intestinal organoids. (C) Expression of the mRNA levels of brush border enzyme genes in 3D and 2D pig intestinal organoids. Data are presented as mean ± standard deviation (n = 5). $0.05 < {}^{\#}p < 0.10$; ${}^{*}p < 0.05$; ${}^{**}p < 0.01$; ${}^{***}p < 0.001$.

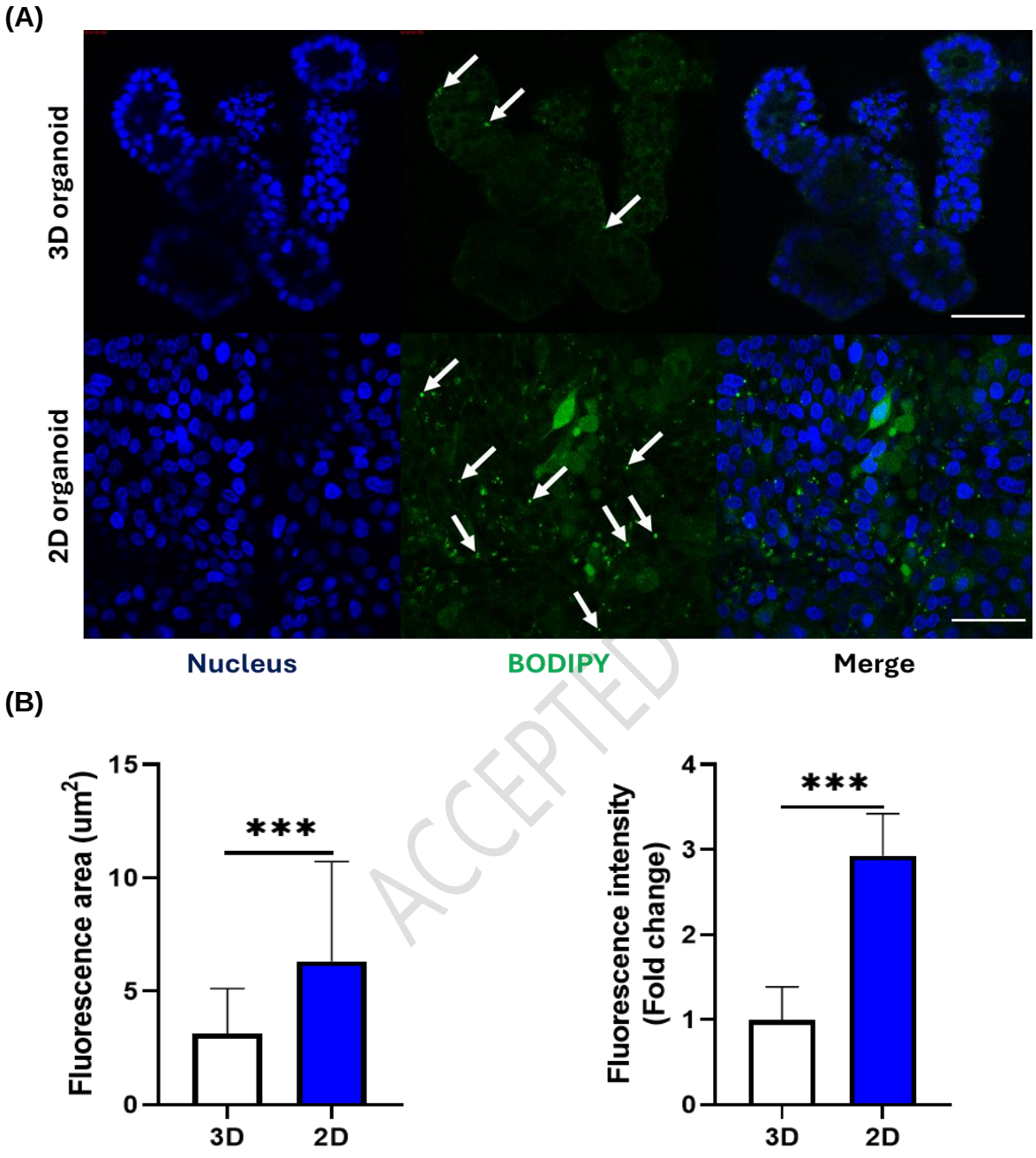

Fig. 4 Fatty acid absorption of 3D and 2D pig intestinal organoids. (A) Representative image of BODIPY-treated 3D and 2D pig intestinal organoids. Nucleus were stained with Hoechst 33342. Scale bar = 50 μm. (B) Quantification of fatty acid analog absorption and fluorescent intensity in 3D and 2D pig intestinal organoids. Data are presented as mean ± standard deviation (3D organoids n = 61, average 4.6 fluorescence area/organoid; 2D organoids n = 145, average 9.6 fluorescence area/image). $^{***}p < 0.001$.

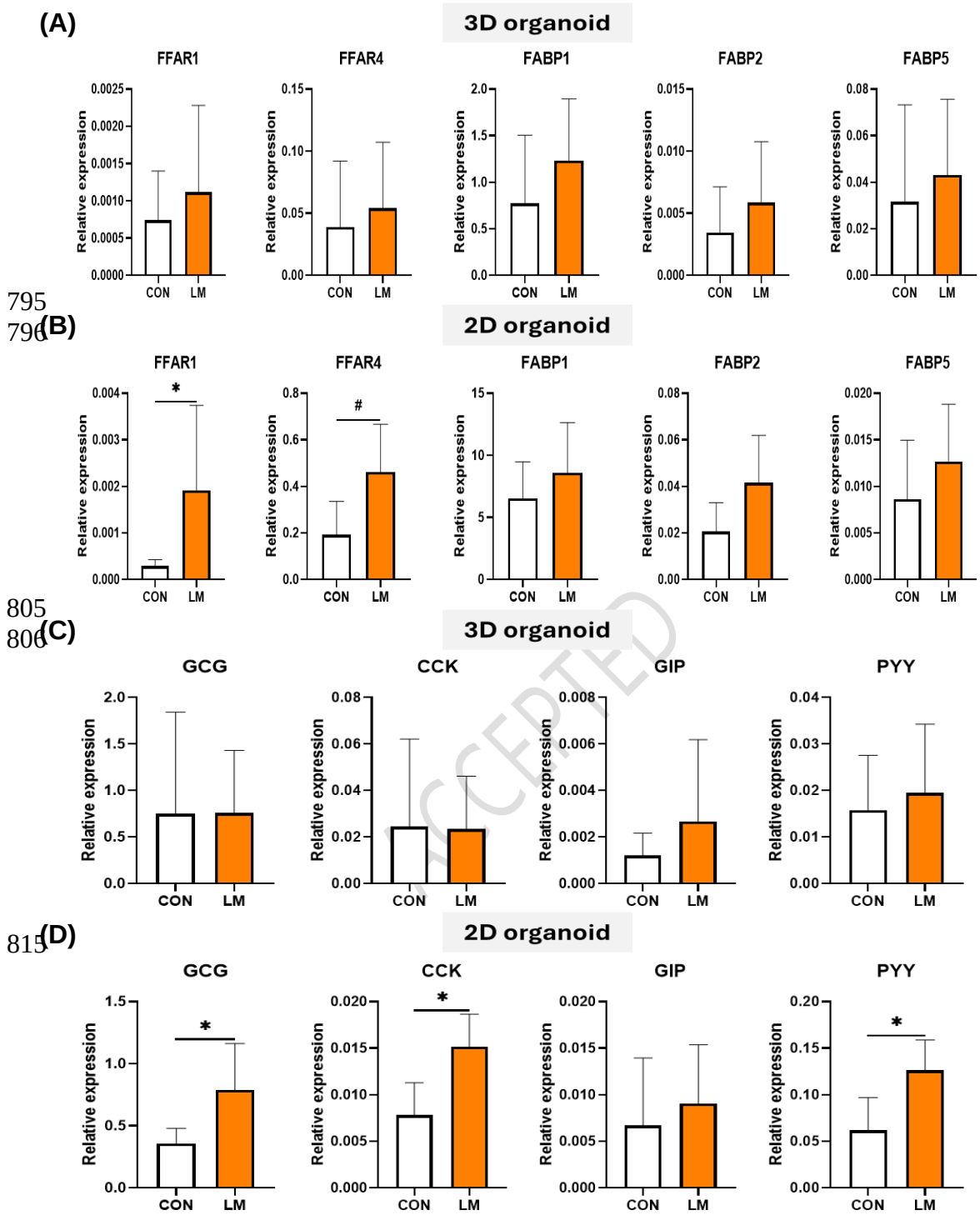

Fig. 5 Different fatty acid-related physiological responses of 3D and 2D pig intestinal organoids. (A) Expression of the mRNA levels of fatty acid receptor and fatty acid binding protein genes in 3D pig intestinal organoids. (B) Expression of the mRNA levels of fatty acid receptor and binding protein genes in 2D pig intestinal organoids. (C) Expression of the mRNA levels of hormone genes in 3D pig intestinal organoids. (D) Expression of the mRNA levels of hormone genes in 2D pig intestinal organoids. Data are presented as mean ± standard deviation (n = 3-5). $0.05 < {}^{\#}p < 0.10$; ${}^{*}p < 0.05$.

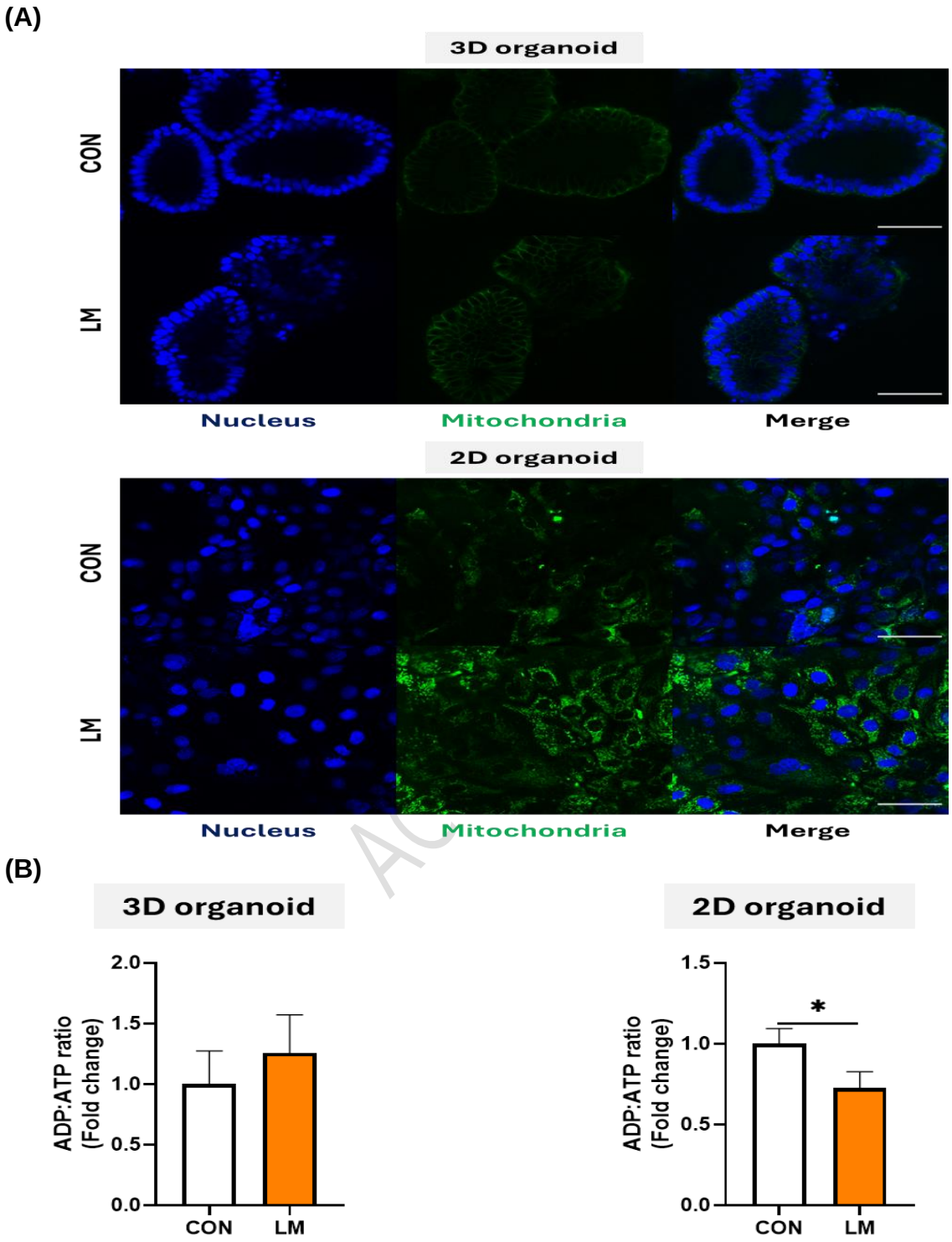

Fig. 6 Fatty acid metabolic responses in 3D and 2D pig intestinal organoids. (A) Representative mitochondria staining image of fatty acid-treated 3D and 2D pig intestinal organoids. Nucleus and mitochondria were stained with Hoechst 33342 and Mitotracker green FM. Scale bar = 50 μm. (B) Relative mitochondrial ADP:ATP ratio of fatty acid-treated 3D and 2D pig intestinal organoids. Data are presented as mean ± standard deviation (n = 3). $^{*}p < 0.05$.